

Unscreened Hartree-Fock calculations for metallic Fe, Co, Ni, and Cu from ab-initio Hamiltonians

I. Schnell,^{1,2} G. Czycholl,² and R. C. Albers¹

¹*Theoretical Division, Los Alamos National Laboratory, Los Alamos, New Mexico 87545*

²*Department of Physics, University of Bremen, P.O.Box 330 440, D-28334 Bremen, Germany*

(Dated: November 6, 2018)

Unscreened Hartree-Fock approximation (HFA) calculations for metallic Fe, Co, Ni, and Cu are presented, by using a quantum-chemical approach. We believe that these are the first HFA results to have been done for crystalline 3d transition metals. Our approach uses a linearized muffin-tin orbital calculation to determine Bloch functions for the Hartree one-particle Hamiltonian, and from these obtains maximally localized Wannier functions, using a method proposed by Marzari and Vanderbilt. Within this Wannier basis all relevant one-particle and two-particle Coulomb matrix elements are calculated. The resulting second-quantized multi-band Hamiltonian with ab-initio parameters is studied within the simplest many-body approximation, namely the unscreened, self-consistent HFA, which takes into account exact exchange and is free of self-interactions. Although the d-bands sit considerably lower within HFA than within the local (spin) density approximation L(S)DA, the exchange splitting and magnetic moments for ferromagnetic Fe, Co, and Ni are only slightly larger in HFA than what is obtained either experimentally or within LSDA. The HFA total energies are lower than the corresponding LSDA calculations. We believe that this same approach can be easily extended to include more sophisticated ab-initio many-body treatments of the electronic structure of solids.

PACS numbers: 71.10.Fd, 71.15.AP, 71.15.Mb, 71.20.Be, 71.45.Gm, 75.10.Lp

I. INTRODUCTION

In this paper we use a quantum-chemical approach to present unscreened Hartree-Fock approximation (HFA) calculations of metallic Fe, Co, Ni, and Cu. Because our approach uses localized Wannier functions, it is a Hubbard-like method that should be easily generalized to include more sophisticated many-body treatments of correlation effects. Nonetheless, it is useful to understand what a HFA method would give before moving on to consider correlation. To place these calculations in context it is useful to briefly review the status of electronic-structure calculations in solids.

Most existing ab-initio (first-principles) methods for the numerical calculation of the electronic properties of solids are based on density functional theory (DFT)¹, which in principle is exact and properly takes into account many-body effects involving the Coulomb interaction between the electrons; for an overview on the present status of DFT we refer to the books^{2,3}. But, in general, the functional dependence of the kinetic energy and the exchange and correlation part of the Coulomb (interaction) energy on the electron density are not known explicitly, and hence additional approximations and assumptions are necessary. A well established additional approximation is the local density approximation (LDA)⁴ (or local spin-density approximation, LSDA, for magnetic systems), which assumes that the exchange-correlation potential depends only on the electronic density locally. Even then, the functional dependence of the exchange-correlation energy on the density is not known in general, and it is usually necessary to make an ansatz for the exchange-correlation functional, which is based on the

homogeneous electron gas. The LDA goes beyond the simplest electron-gas approximation, the HFA, in that correlation energy is explicitly taken into account. On the other hand, the exact HFA exchange potential is non-local, an effect which the local LDA exchange potential misses. However, in practice LDA-treatments are simpler than HFA-calculations, because local exchange is easier to treat than non-local exchange, and are usually in better agreement with experiment. Therefore, DFT-(LDA-like) treatments have been far more common than HFA during the past few decades, even in quantum chemistry (with a long tradition of methods based on HFA).

Ab-initio DFT-LDA calculations have been very successful for many materials and ground-state properties such as crystal structure, ground state and ionization energy, lattice constant, bulk modulus, crystal anharmonicity⁵, magnetic moments, and some photo emission spectra. However, there are also important limitations. For example, LDA predicts a band gap for semiconductors that is almost a factor of two too small, while the HFA overestimates the band gap for semiconductors⁶. In addition, for many strongly correlated (narrow energy band) systems such as high-temperature superconductors, heavy fermion materials, transition-metal oxides, and 3d itinerant magnets, the LDA is usually not sufficient for an accurate description (predicting metallic rather than semiconducting behavior, failing to predict quasi-atomic-like satellites, etc).

Therefore, it is important to look for ab-initio methods and improvements that go beyond L(S)DA. Recently there have been several attempts to combine ab-initio LDA calculations with many-body approximations.^{7,8,9,10,11,12,13,14,15,16} All of these recent

developments add local, screened Coulomb (Hubbard) energies U between localized orbitals to the one-particle part of the Hamiltonian obtained from an ab-initio LDA band-structure calculation, but differ in how they handle the correlation part. These approaches, have in common that they have to introduce a Hubbard U as an additional parameter and hence are not really first-principles treatments. Although they use an LDA ab-initio method to obtain a realistic band structure, i.e., single-particle properties, Coulomb matrix elements for any particular material are not known, and the Hubbard U remains an adjustable parameter. In addition, since some correlations are included in LDA as well as by the Hubbard U , it is unclear how to separate the two effects and double-counting of correlation may be included in these approximations.

Other attempts to improve LDA include gradient corrections, non-local density schemes, self-interaction corrections, and the GW approximation (GWA). Gradient corrections¹⁷ approximately account for the fact that the electron density is not constant but \mathbf{r} -dependent in an inhomogeneous electron gas and use an exchange-correlation potential containing $\nabla n(\mathbf{r})$ terms. The non-local density schemes go beyond LDA by considering that the exact exchange-correlation potential $V_{xc}(\mathbf{r})$ cannot depend only on the density $n(\mathbf{r})$ at the same position \mathbf{r} but should depend also on the electron density at all other positions $n(\mathbf{r}')$. Usually the new ansatz for the functional of the exchange-correlation energy contains the pair correlation function or the interaction of the electrons with the exchange-correlation hole.^{17,18} The recently developed exact exchange (EXX) formalism^{19,20} cancels the spurious (unphysical) electronic self-interaction present in LDA and gradient corrected exchange functionals. A standard method for ab-initio calculations of excited states is the GWA^{21,22}. Denoting the one-particle Green function by G and the screened interaction by W , the GWA is an approximation for the electronic selfenergy $\Sigma \approx GW$, which is correct in linear order in W and can diagrammatically be represented by the lowest-order exchange (Fock) diagram. The one-particle Green function G is usually obtained for the effective one-particle LDA Hamiltonian.

The HFA has long been a standard electronic-structure method. Despite its many manifest defects, it is still important to know what such a calculation would predict before turning to more sophisticated approaches for correlation effects. In this paper we provide HFA calculations for Fe, Co, Ni, and Cu using an approach that we hope will be easily generalizable to more sophisticated treatments of correlation.

This is done by using the following steps:

1. Perform a conventional, self-consistent, band-structure calculation for an effective one-particle Hamiltonian, namely, the Hartree Hamiltonian, to obtain a suitable basis set of Bloch functions.
2. By taking into account only a finite number J of

bands one chooses a truncated one-particle Hilbert space. The Marzari-Vanderbilt²³ algorithm is then used to construct a maximally localized set of Wannier functions, which span the same truncated one-particle Hilbert space.

3. All one-particle (tight-binding) and two-particle (Coulomb) matrix elements of the Hamiltonian within this Wannier function basis are calculated.
4. The resulting electronic many-body Hamiltonian in second quantization with parameters determined from first principles is studied within the HFA.

We use the “linear muffin-tin orbital” (LMTO) method²⁴ within the “atomic-sphere approximation” (ASA)²⁵ to perform the band-structure calculation for the Hartree Hamiltonian in first quantization. The second step of constructing localized Wannier functions is important, since then both the tight-binding and Coulomb matrix elements should be important only on-site and for a few neighbor shells (the most natural mapping to standard Hubbard-like models). The direct Coulomb matrix elements of the maximally localized Wannier basis are rather large, about 20 eV in magnitude. Our results are compared with those obtained from a standard LSDA calculation.^{2,3,26,27} Although the 3d-bands and the 4s-band overlap in the L(S)DA approximation, our unscreened HFA calculations give 3d-bands that lie considerably lower (between 10 and 20 eV) than the 4s-band. The HFA correctly predicts ferromagnetism for the ferromagnetic metals Fe, Co, and Ni and no magnetism for Cu, but with a much larger exchange splitting between majority and minority 3d bands than obtained within LSDA and with a slightly larger magnetic moment per site than obtained experimentally or within LSDA. The total energy is lower in HFA than in LSDA. The LSDA results for metals are probably more reliable than our HFA results, which lack important screening and correlation effects. In order for our method to go beyond LSDA we would need to use better many body methods than the (unscreened) HFA, which should be possible within our scheme.

To the best of our knowledge we do not know of any other published HFA results (band structure, density of states, magnetism, magnetic moment, total energy, etc.) for the 3d ferromagnets Fe, Co and Ni, unless it was implicitly applied to these materials for schemes like the local ansatz²⁸, where HFA results serve as an input to higher order calculations. This is not surprising since the HFA has, from very early on, been viewed as a poor approximation for metals. For example, when applied to the homogeneous electron gas (as the simplest model of an infinite metallic system), the HFA has well-known Fermi edge singularities^{29,30}. These lead, in particular, to a vanishing density of states (DOS) at the Fermi energy, which is, of course, unphysical. This unphysical feature usually prevails in actual HFA-calculations for real metals³¹, though sometimes this singularity is hard

to see in actual HFA-results³². In our calculations the non-locality is handled through the calculation of expectation values (matrix elements of the density matrix), which makes HF calculations as easy as Hartree calculations. Furthermore, because of our localized Wannier basis, we only keep on-site and next neighbor Coulomb and exchange matrix elements. Hence our calculations have an effective short-ranged Coulomb interaction. Although longer-range Coulomb matrix elements are small in our calculations, which is why we truncate them, it is possible that if all of them were kept to infinite distances that they could add up to give Fermi edge singularities (which are due to the long-ranged nature of the bare Coulomb interaction) and other standard anomalies. Correlation or screening would quickly kill these effects.

The approximation closest to HF is the exact exchange formalism (EXX)^{19,20} mentioned earlier. The EXX method is different from the LDA only in that the EXX energy²⁰, rather than the LDA exchange energy, is used; thus, LDA correlations are still present. The EXX energy, which corresponds to the Fock term in the HFA, is treated as a functional of electron density and the method is also (like HF) self-interaction-free. Although the EXX would appear to be very similar to HF, the EXX-only method^{33,34}, which does not include any correlation, gives the dispersion of noninteracting electrons instead of the HF dispersion when applied to the homogeneous electron gas, while their total energies are exactly the same. For atoms the EXX-only method gives total energies that agree well with HF. Due to these similarities, we will compare our results with EXX where possible. One should note, however, that most EXX calculations include a local correlation potential.

The paper is organized as follows. In Section II, we briefly summarize some basic notation, give the Hamiltonian in first and second quantization, and describe our LMTO-Hartree calculations and our Wannier basis functions. Results for the matrix elements, in particular, the direct Coulomb and exchange matrix elements are given in Section III; we also compare these results with calculations of the Slater integrals. The application of the (unscreened) HFA to the multi-band Hamiltonian in second quantization is the subject of Section IV. For an interpretation of the results we compare the numerical HFA results obtained for the crystal with previous atomic HFA results and with numerical and analytical results for a simplified local atomic model in Section V. A comparison with the more standard LSDA as well as EXX results follows in Section VI, before the paper closes with a short discussion.

II. HAMILTONIAN AND BASIS FUNCTIONS

A system of N_e interacting (non-relativistic) electrons can be described by the Hamiltonian

$$H = T + V + W = \sum_{i=1}^{N_e} \frac{\mathbf{p}_i^2}{2m} + \sum_{i=1}^{N_e} V(\mathbf{r}_i) + \sum_{i>j} \frac{e^2}{|\mathbf{r}_i - \mathbf{r}_j|} . \quad (1)$$

The first part T is the kinetic energy of the electrons. The $V(\mathbf{r})$ describes the external one-particle potential. The formalism of “second quantization”, automatically accounts for the antisymmetry through the fermion anticommutation relations. In second quantization the full many-body Hamiltonian can be written as:

$$H = \sum_{i,j,\sigma} t_{ij} c_{i\sigma}^\dagger c_{j\sigma} + \frac{1}{2} \sum_{i,j,k,l,\sigma,\sigma'} W_{ij,kl} c_{i\sigma}^\dagger c_{j\sigma'}^\dagger c_{k\sigma'} c_{l\sigma} \quad (2)$$

Here i, j, k, l denote a complete set of one-particle orbital quantum numbers and σ, σ' are the spin quantum numbers. The states $|i\rangle$ and the corresponding wave functions $\varphi_i(\mathbf{r}) = \langle \mathbf{r} | i \rangle$ form a basis of the one-particle Hilbert space. The matrix elements in Eq. 2 of course depend on the one-particle basis $\{|i\rangle\}$ that is chosen. But because of the completeness relation the physical results should, not depend on the choice of the one-particle basis. Because of the lattice periodicity an obvious choice for a one-particle basis is a Bloch basis $\{|n\mathbf{k}\rangle\}$; then the orbital one-particle quantum numbers n, \mathbf{k} are the band index n and the wave number \mathbf{k} (within the first Brillouin zone). In practice, one can work only on a truncated, finite-dimensional one-particle Hilbert space. Here the truncation consists of including only a finite number of bands and a set of \mathbf{k} -values from a discrete mesh in \mathbf{k} -space. But, because the Bloch states are delocalized, a very large number of Coulomb matrix elements (depending on four quantum numbers) between all possible \mathbf{k} -states would have to be calculated. Therefore, it seems that a more appropriate basis would be to use well localized wave functions, where it is expected that a short-range tight-binding assumption will hold, i.e., that the on-site and the inter-site matrix elements for only a few neighbor shells are sufficient. The Wannier states are related to the Bloch states by the unitary transformations:

$$w_{\mathbf{R}n}(\mathbf{r}) = \langle \mathbf{r} | \mathbf{R}n \rangle = \frac{1}{N} \sum_{\mathbf{k}} e^{-i\mathbf{k}\mathbf{R}} \psi_{n\mathbf{k}}(\mathbf{r}) \quad (3)$$

$$|\psi_{n\mathbf{k}}\rangle = \sum_{\mathbf{R}} e^{i\mathbf{k}\mathbf{R}} |\mathbf{R}n\rangle$$

Now our strategy is the following:

- Perform a traditional band-structure calculation for an effective one-particle Hamiltonian H_{eff} with lattice periodicity to obtain a Bloch basis of the Hilbert space. Only a finite number of band indices will be considered and the calculations will be done for a discretized, finite mesh in \mathbf{k} -space, i.e., we will work only on a reduced, truncated Hilbert space.

- Determine well-localized Wannier functions spanning the same (truncated) Hilbert space as the Bloch basis from the canonical transformation (3) described above.

Of course, the important energy bands (and corresponding band indices) are those that determine the electronic properties of the system, i.e., the bands near to the Fermi level. Because the Hilbert space is truncated, we do no longer work with a complete basis set. Hence, it is important to start from Bloch functions obtained from a band-structure calculation for a well chosen effective one-particle Hamiltonian. The simplest choice would be the bare one-particle potential $V(\mathbf{r})$. However, without any Coulomb repulsion the 3d-states become very strongly bound atomic-like (core) states, which would be pushed well below the Fermi energy, and therefore the corresponding Bloch eigenfunctions are not a good starting point to describe the electronic bands close to the Fermi level. Because the Hilbert space is truncated, it is extremely important to start from a band Hamiltonian $T + V_{\text{eff}}$ that gives eigenfunctions as close as possible to those which are expected to form the relevant many-body states of the interacting system. The bare one-particle potential is consequently a bad choice. Therefore, we choose the Hartree Hamiltonian, which already accounts for effects of the Coulomb interaction in the mean-field approximation. Therefore, the eigenenergies (energy bands) will be about the right magnitude and the resulting basis functions can be expected to be more suitable in the energy regime around the Fermi level. Then the Bloch basis is obtained by solving the one-particle Schrödinger equation

$$\left(\frac{\mathbf{p}^2}{2m} + V(\mathbf{r}) + V_{\text{H}}(\mathbf{r})\right)\psi_{n\mathbf{k}}(\mathbf{r}) = \varepsilon_n(\mathbf{k})\psi_{n\mathbf{k}}(\mathbf{r}) \quad (4)$$

where the Hartree potential is given by

$$V_{\text{H}}(\mathbf{r}) = \int d^3r' \frac{e^2 \rho(\mathbf{r}')}{|\mathbf{r} - \mathbf{r}'|} . \quad (5)$$

Since the only purpose in solving the effective one-particle Schrödinger equation (4) is the construction of a suitable basis set of Bloch functions, we will not make use of the eigenenergies $\varepsilon_n(\mathbf{k})$ obtained in Eq. 4. Note that the Hartree potential, and hence our basis, is independent of spin. Nevertheless we can (in the following) expand the spin dependent HF Hamiltonian in this basis.

For the materials of interest we performed a self-consistent Hartree band-structure calculation. Besides the nuclear charge we used the (experimentally) known results for the lattice structure (bcc for Fe, fcc otherwise; Co should actually be hexagonal) and for the lattice constant as input. For the band-structure calculation we used the LMTO-ASA method^{24,25} within the atomic sphere approximation (ASA). We have used the frozen core approximation²⁵, i.e. only treated the valence electrons as actual bands, while leaving the core electrons “frozen”. For the radius of the overlapping muffin-tin

spheres, the Wigner-Seitz radius S , we used: $S = 2.662a_0$ for Fe, $S = 2.621a_0$ for Co, $S = 2.602a_0$ for Ni and $S = 2.669a_0$ for Cu (Ref. 25). Within the muffin-tin spheres the potential and wave functions are expanded in spherical harmonics with a cutoff $l_{\text{max}} = 2$, i.e., s, p, and d-orbitals are included, which limits the calculation to 9 bands for one atom per unit cell.

In Ref. 35, we describe how maximally localized Wannier functions can be calculated from LMTO Bloch wave functions using a method proposed by Marzari and Vanderbilt, which is described in detail in Ref. 23. The Wannier functions are admixtures having different angular contributions (3d, 4s, 4p). Since the original Bloch functions from which the Wannier functions are constructed were given in terms of a spherical harmonics expansion, the new Wannier functions (and their contribution in each individual muffin-tin sphere) can also be decomposed into these spherical harmonics contributions

$$w_n(\mathbf{R}; \mathbf{r}) = \sum_L \left\{ \phi_{\nu l}(r) A_L^{\mathbf{R}n} + \dot{\phi}_{\nu l}(r) B_L^{\mathbf{R}n} \right\} Y_L(\hat{\mathbf{r}}) . \quad (6)$$

One can then calculate the weight of the contributions to the Wannier function (centered at $\mathbf{0}$) within the different muffin-tin spheres

$$\langle w_n | w_n \rangle_{\mathbf{R}} \equiv \int_{\mathbf{R}} d^3\mathbf{r} |w_n(\mathbf{r})|^2 = \int_{\mathbf{0}} d^3\mathbf{r} |w_n(\mathbf{R}; \mathbf{r})|^2 , \quad (7)$$

and one can also decompose this into the different l -contributions according to:

$$\langle w_n | w_n \rangle_{\mathbf{R}} = \sum_l \underbrace{\sum_{m=-l}^l \left\{ |A_{lm}^{\mathbf{R}n}|^2 + \langle \dot{\phi}_{\nu l}^2 \rangle |B_{lm}^{\mathbf{R}n}|^2 \right\}}_{\equiv C_l^{\mathbf{R}n}} \quad (8)$$

For the 3d-system iron these quantities are tabulated in Table I. The first line is the weight $\langle w_n | w_n \rangle_{\mathbf{0}}$ in the center muffin-tin. Between 88 and 98% of the total weight of the Wannier functions is to be found already within the center muffin-tin; this shows how well localized our Wannier functions are with the lowest five functions having values of more than 95%. Rows 2–4 in this table indicate the different l -contribution or l -character of the Wannier functions. One sees that the optimally localized Wannier functions are not pure within their l -character, but the lowest five Wannier functions (0-4) still have mainly $l = 2$ (3d) character. Higher band-index states (which are slightly less well localized according to row 1) are admixtures that have mainly $l = 1$ (4p) character (about 50 %), but also a considerable amount of $l = 0$ (4s) and $l = 2$ (3d) character. Corresponding results for the other 3d-systems Co, Ni, and Cu are similar and, therefore, not repeated here. Our detailed results are given in Ref. 27.

n	0	1	2	3	4	5	6	7
$\sum_l C_l^{0n}$.9761	.9765	.9596	.9800	.9773	.8754	.8731	.8763
$\sum_{\mathbf{R}} C_{l=0}^{\mathbf{R}n}$.0019	.0018	.0081	.0019	.0017	.2224	.2381	.2265
$\sum_{\mathbf{R}} C_{l=1}^{\mathbf{R}n}$.0955	.0726	.1797	.0611	.0728	.5480	.5509	.5347
$\sum_{\mathbf{R}} C_{l=2}^{\mathbf{R}n}$.9026	.9256	.8121	.9370	.9255	.2295	.2110	.2388

TABLE I: Some properties of the lowest eight maximally localized Wannier functions of Fe.

III. ONE PARTICLE AND COULOMB MATRIX ELEMENTS

From the optimally localized Wannier functions we calculate the one-particle matrix elements

$$t_{12} = \int d^3\mathbf{r} w_1^*(\mathbf{r}) \left(-\frac{\hbar^2}{2m} \nabla^2 + V(\mathbf{r}) \right) w_2(\mathbf{r}) \quad (9)$$

and the Coulomb matrix elements of the Hamiltonian

$$W_{12,34} = \int d^3\mathbf{r} d^3\mathbf{r}' w_1^*(\mathbf{r}) w_2^*(\mathbf{r}') \frac{e^2}{|\mathbf{r} - \mathbf{r}'|} w_3(\mathbf{r}') w_4(\mathbf{r}) . \quad (10)$$

Here we use the abbreviated notation 1 to mean $\mathbf{R}_1 n_1$ and 2 to mean for $\mathbf{R}_2 n_2$, etc. In Ref. 35, we have described how these matrix elements can be evaluated. Concerning the Coulomb matrix elements, we have used the two different numerical algorithms proposed in Ref. 35 for their evaluation, namely the FFT-algorithm and a spherical expansion algorithm. The latter method makes use of the fact that (in each muffin-tin sphere) the Wannier functions are explicitly given as linear combinations of products of spherical harmonics and a radial wave function. The expansion

$$\frac{1}{|\mathbf{r} - \mathbf{r}'|} = \sum_{k=0}^{\infty} \frac{4\pi}{2k+1} \frac{r_{<}^k}{r_{>}^{k+1}} \sum_{m=-k}^k Y_K^*(\hat{\mathbf{r}}') Y_K(\hat{\mathbf{r}}) \quad (11)$$

($K = \{k, m\}$) makes it possible to express the on-site Coulomb integrals as one-dimensional integrals over products of the radial functions and Gaunt coefficients. The results obtained by this algorithm and by the independent FFT-algorithm agree within errors of at most 1%. Since our basis functions are well-localized, we may truncate the tight-binding and Coulomb matrix elements. We only consider on-site and next neighbor matrix elements, by next neighbor Coulomb matrix elements, we mean matrix elements for which the four sites (appearing in the indices) are (pairwise) maximally a next neighbor distance apart.

Results for the on-site direct and exchange Coulomb matrix elements between the optimally localized Wannier functions are given in Table II for iron. The direct Coulomb integrals $U_{nm} = W_{nm,nn}$ between the Wannier states with the lowest five band indices ($n, m \in \{0, \dots, 4\}$), which according to the Table I have mainly 3d-character, are rather large, up to 23 eV for Fe. Within

U_{nm}	0	1	2	3	4	5	6	7	8
0	22.42	20.90	20.10	20.96	20.86	14.16	13.32	13.96	13.50
1	20.90	23.04	19.95	21.55	21.53	14.07	13.54	13.58	14.15
2	20.10	19.95	20.77	20.05	19.83	12.95	13.46	13.37	13.22
3	20.96	21.55	20.05	23.27	21.67	13.46	14.05	13.98	13.98
4	20.86	21.53	19.83	21.67	22.99	13.71	13.28	14.25	14.12
5	14.16	14.07	12.95	13.46	13.71	13.67	9.45	9.58	9.64
6	13.32	13.54	13.46	14.05	13.28	9.45	13.52	9.27	9.50
7	13.96	13.58	13.37	13.98	14.25	9.58	9.27	13.75	9.65
8	13.50	14.15	13.22	13.98	14.12	9.64	9.50	9.65	13.81

J_{nm}	0	1	2	3	4	5	6	7	8
0	22.42	0.84	0.61	0.75	0.99	0.86	0.73	0.81	0.42
1	0.84	23.04	0.77	0.88	0.84	0.70	0.51	0.48	0.86
2	0.61	0.77	20.77	0.88	0.70	0.96	0.93	0.92	0.60
3	0.75	0.88	0.88	23.27	0.82	0.33	0.78	0.64	0.69
4	0.99	0.84	0.70	0.82	22.99	0.52	0.46	0.75	0.83
5	0.86	0.70	0.96	0.33	0.52	13.67	0.58	0.56	0.57
6	0.73	0.51	0.93	0.78	0.46	0.58	13.52	0.45	0.56
7	0.81	0.48	0.92	0.64	0.75	0.56	0.45	13.75	0.55
8	0.42	0.86	0.60	0.69	0.83	0.57	0.56	0.55	13.81

TABLE II: On-site direct and exchange Coulomb matrix elements between Wannier functions for Fe. All energies are in eV's.

the 3d-like bands the inter-band direct Coulomb matrix elements are of the same magnitude as the intra-band matrix elements. The matrix elements between 3d-states and 4sp-states are considerably smaller, of the magnitude of 13 - 14 eV. For electrons in 4sp-states ($n, m \in \{5, \dots, 9\}$) the direct intra-band Coulomb matrix elements are again of the order of 13 - 14 eV, but the inter-band matrix elements are slightly smaller, about 9 eV. The exchange matrix elements $J_{nm} = W_{nm,nn}$ are always much smaller, usually less than 1 eV (for $n \neq m$). The corresponding results for the other 3d-systems investigated (Co, Ni and Cu) are very similar.²⁷

	U	J	t_{NN}	t_{NNN}
Fe	21.1	.81	.59	.24
Co	22.6	.87	.55	.10
Ni	22.6	.88	.75	.11
Cu	24.5	.94	.80	.12

TABLE III: Averaged on-site Coulomb, exchange, nearest neighbor and next nearest neighbor hopping matrix elements for the 4 3d-systems; energies are in eV.

For the 5 states with predominant 3d-character we have calculated the averages of the on-site direct and

exchange Coulomb matrix elements

$$U \equiv \frac{1}{25} \sum_{mm'} W_{mm'm'm} \quad (12)$$

$$J \equiv \frac{1}{20} \sum_{m \neq m'} W_{mm'mm'} \quad , \quad (13)$$

as well as the averages of the absolute values of the nearest neighbor (NN) and next nearest neighbor (NNN) hopping matrix elements

$$t_{NN(N)} \equiv \frac{1}{25} \sum_{n,m} |t_{\mathbf{R}nm}| \quad . \quad (14)$$

The results obtained thereby for the 4 transition metals under consideration are shown in Table III. The U-values vary between 21 eV for Fe and 25 eV for Cu, the J-values are smaller than 1 eV and the hopping matrix elements are of the magnitude 0.5 – 0.7 eV for nearest-neighbor (NN) and 0.1 – 0.2 eV for next nearest neighbor (NNN), and further on decrease with increasing distance.

	F^0	F^2	F^4
Fe (crystal)	21.62	9.61	5.91
Fe (atom [37])	23.76	10.96	6.81
Co (crystal)	23.18	10.31	6.34
Co (atom [37])	25.15	11.58	7.20
Ni (crystal)	24.69	11.00	6.77
Ni (atom [37])	26.53	12.20	7.58
Cu (crystal)	26.27	11.72	7.23
Cu (atom [37])	27.90	12.82	7.96

TABLE IV: Slater integrals F^k (in eV) for the 3d-systems Fe, Co, Ni, Cu as obtained by our calculations and within an earlier atomic calculation³⁷.

We have also evaluated the Slater integrals³⁶:

$$F^k \equiv e^2 \int dr r^2 \int dr' r'^2 |R_{l=2}(r)|^2 \frac{r^k}{r^{k+1}} |R_{l=2}(r')|^2 \quad , \quad (15)$$

where $R_{l=2}(r)$ is a radial (atomic) d-wave function (obtained by solving the Schrödinger equation for a radial symmetric potential, for instance). Note that only the three integrals F^0 , F^2 and F^4 are required to determine all the Coulomb d -matrix elements. Using the radial d -wave function obtained from the Hartree calculation we obtain the following values for the Slater integrals of the four 3d-systems: $F^0 = 21.62$ eV for Fe, 23.18 eV for Co, 24.69 eV for Ni, and 26.27 eV for Cu. This means, the Slater integrals F^0 are rather good estimates of our (averaged) Coulomb matrix elements. These values are also in agreement with older results obtained in calculations for 3d-atoms³⁷. In Table IV we show our F^k -values for the four 3d-crystals and compare them with corresponding atomic calculations from Ref. 37. Obviously, there is fairly good agreement between these atomic and our results.

IV. UNSCREENED HARTREE-FOCK APPROXIMATION

After we have determined the matrix elements within our restricted basis set of 9 maximally localized Wannier functions (per site and spin), we have a Hamiltonian in second quantization of the form

$$H = \sum_{12\sigma} t_{12} c_{1\sigma}^\dagger c_{2\sigma} + \frac{1}{2} \sum_{1234\sigma\sigma'} W_{12,34} c_{1\sigma}^\dagger c_{2\sigma'}^\dagger c_{3\sigma'} c_{4\sigma} \quad (16)$$

for which all the matrix elements are known from first principles. The simplest approximation one can now apply is the HFA, which replaces the many-body Hamiltonian by the effective one-particle Hamiltonian

$$H_{\text{HF}} = \sum_{12\sigma} (t_{12} + \Sigma_{12,\sigma}^{\text{HF}}) c_{1\sigma}^\dagger c_{2\sigma} \quad (17)$$

$$\begin{aligned} \text{with } \Sigma_{12,\sigma}^{\text{HF}} &= \Sigma_{12}^{\text{Hart}} + \Sigma_{12,\sigma}^{\text{Fock}} \quad (18) \\ &= \sum_{34\sigma'} [W_{13,42} - \delta_{\sigma\sigma'} W_{31,42}] \langle c_{3\sigma'}^\dagger c_{4\sigma'} \rangle \quad . \end{aligned}$$

Here the expectation values $\langle c_{1\sigma}^\dagger c_{2\sigma} \rangle$ have to be determined self-consistently for the HF Hamiltonian (17). Note that the Fock (exchange) term is spin (σ) dependent and may, therefore, give rise to magnetic solutions.

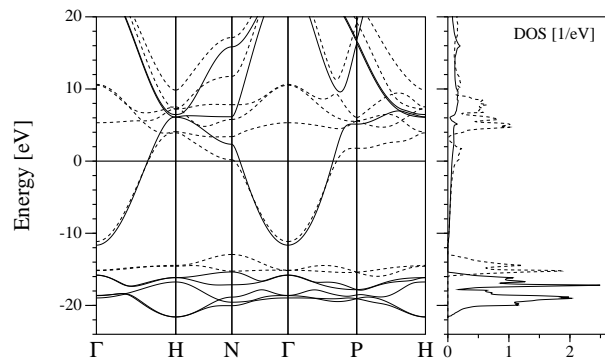


FIG. 1: Hartree-Fock band-structure and density of states (per spin) of Fe; the full line shows the majority (spin up), the dashed line the minority spin component.

	HF	EXX	LSDA	Experiment
Fe	2.90	3.27	2.18	2.22
Co	1.90	2.29	1.58	1.72
Ni	0.76	0.68	0.58	0.62

TABLE V: Spin magnetic moments (μ_B /atom) from different methods. The EXX results are from Ref. 40.

The Hartree-Fock results for the four materials of interest are shown in Figs. 1–4. We show the effective HF band structure and its density of states (DOS). In our HF calculations there are no singularities (or a vanishing DOS) at the Fermi level since we start from a

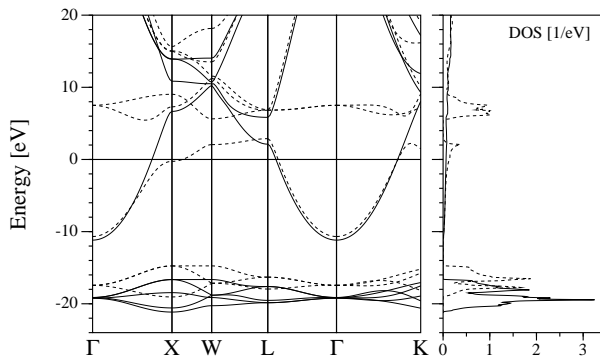


FIG. 2: Hartree-Fock band-structure and density of states (per spin) of Co; the full line shows the majority (spin up), the dashed line the minority spin component.

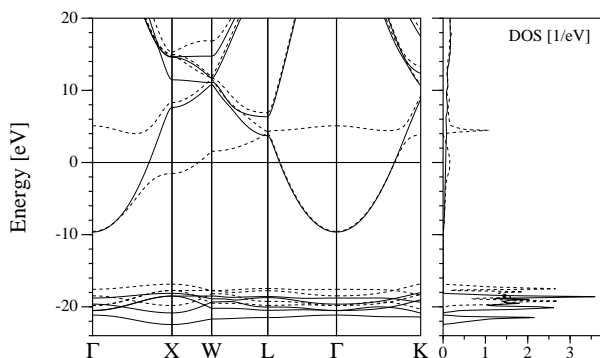


FIG. 3: Hartree-Fock band-structure and density of states (per spin) of Ni; the full line shows the majority (spin up), the dashed line the minority spin component.

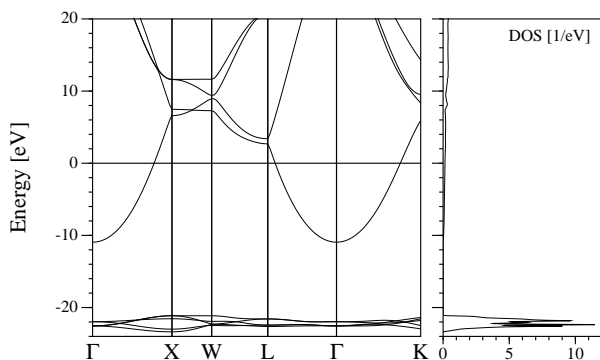


FIG. 4: Hartree-Fock band-structure and density of states (for both degenerate spin directions) of Cu.

localized description and consider the Coulomb matrix elements only up to next neighbors. Therefore, we implicitly truncate the Coulomb interaction in real space and in practice work with an effective short-ranged interaction. Within HFA the main part of the 3d-bands lies between 18 and 22 eV below the Fermi level and is separated from the 4sp-bands. We find magnetism in

HFA for Fe, Co, and Ni in agreement with experiment. The five majority spin d-bands are about 20 eV below the Fermi energy and are completely filled. But the partially filled minority d-bands have two (for Fe), three (for Co), and four (for Ni) filled bands between -18 and -15 eV, and the rest are around and above the Fermi level. The resulting magnetic moments are shown in Table V. For copper no magnetism and exchange splitting of the 3d-bands is obtained, but the (spin degenerate) 3d-bands are at about 22 eV below the Fermi level and separated from the 4sp-bands. If we compare these results with the results of the simple Hartree approximation, which are qualitatively similar to LDA results (as shown e.g. in Ref. 26, or in our detailed results²⁷), we see that the exchange term has two effects: It produces an exchange splitting and the possibility of magnetic solutions, and it draws the 3d-bands energetically down by an amount of about 20 eV. Compared with experiment the HFA overestimates magnetism and leads to overly large values for the magnetic moment, see Table V. This is consistent with Heisenberg or Ising model studies where the mean-field approximation HFA also has the tendency to overestimate magnetism and magnetic solutions. However, the reason why the 3d-bands lie so far below the Fermi level and the 4sp-band in HFA has nothing to do with the existence and overestimation of magnetism. This can be seen already from the non-magnetic system Cu, for which the (fully occupied) 3d-bands also lie at about 22 eV below the Fermi level (see Fig. 4). To demonstrate this also for a system with a partially filled 3d-band we have done a non-magnetic Hartree-Fock calculation for Co (by forcing equal occupation for both spin directions). The results for the band structure and the DOS are shown in Fig. 5. We observe again that the main part of the 3d-bands are well below the 4s-bands and Fermi level; note the hybridization gap caused by the unoccupied 3d-bands above the Fermi level.

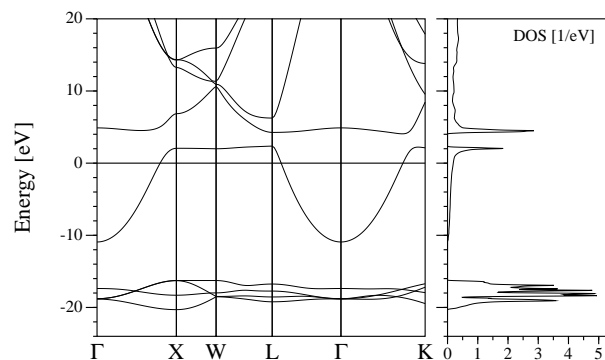


FIG. 5: Non-magnetic Hartree-Fock band-structure and density of states (for both degenerate spin directions) of Co.

V. COMPARISON WITH ATOMIC HARTREE-FOCK RESULTS

We have seen in the previous section that one effect of the HFA calculation, when compared with the Hartree calculation, is the shift of the 3d-bands down (about 20 eV below the Fermi level and about 8–10 eV below the bottom of the 4sp-band). This shift of the d-bands is about the same energy as the Coulomb matrix elements U , and roughly agrees with earlier atomic Hartree-Fock calculations^{37,38}, where the 3d-states are also about 10 eV below the 4s-states.

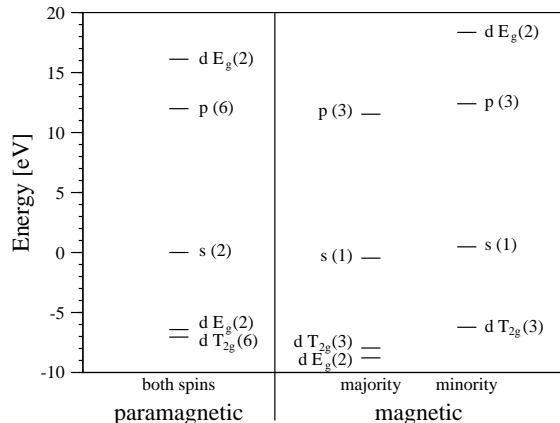


FIG. 6: Energy eigenvalues from quasi-atomic HFA-calculation. The numbers in brackets indicate the degeneracy.

Because the inter-site hopping matrix elements in Table III are much smaller than the U -values one may consider an expansion in t/U , with the zeroth order approximation to completely neglect hopping. Doing this, we have performed a quasi-atomic HFA calculation for Co, by including only the on-site one-particle and two-particle (Coulomb) matrix elements. The results are summarized in Fig. 6; the degeneracy of the different levels is also indicated. In the paramagnetic case, we find that the 3d-bands are below the 4s-bands (at the Fermi level) by about 6 to 7 eV, which is in rough agreement with the earlier atomic HFA results^{37,38}. The splitting between the occupied and unoccupied 3d-states is about 23 eV, which is the on-site U for Co. Magnetic HFA solutions are also found in the atomic limit for Co, as shown in the right panel of Fig. 6. The majority-spin 3d states (T_{2g} and E_g) are now completely filled and energetically lie lower than the corresponding non-magnetic HFA-states. But only the (3-fold degenerate) T_{2g} -states of the minority-spin electrons are filled whereas the E_g -states of the minority electrons are empty (and now even 26 eV above the occupied d-states). The additional energetical shifts between the occupied 3d-states in the paramagnetic and ferromagnetic atomic HFA solution are due to the exchange matrix elements J .

This behavior can qualitatively be understood within the framework of the following simple, analytically solv-

able model. Similar to the numerical HFA-results presented and discussed above, we neglect all inter-site one-particle (hopping) and interaction matrix elements. Furthermore, we assume that we have diagonalized the one-particle Hamiltonian, taking into account only the atomic 3d-levels and assuming that the on-site one-particle diagonal matrix elements ε , the Coulomb matrix elements U , and the exchange matrix elements J are equal, i.e., that the 3d-levels are degenerate in the atomic limit with no crystal-field effects. Then the atomic part of the many-body Hamiltonian can be written as

$$H = \sum_{i\sigma} \varepsilon c_{i\sigma}^\dagger c_{i\sigma} + \frac{U}{2} \sum_{(i\sigma) \neq (j\sigma')} c_{i\sigma}^\dagger c_{i\sigma} c_{j\sigma'}^\dagger c_{j\sigma'} + \frac{J}{2} \sum_{i \neq j, \sigma \sigma'} c_{i\sigma}^\dagger c_{j\sigma'}^\dagger c_{i\sigma'} c_{j\sigma} \quad (19)$$

where $i, j \in \{0, \dots, 4\}$ denote the 5 (degenerate) 3d-states.

The standard Hartree-Fock decoupling leads to

$$H = \sum_{i\sigma} \left(\varepsilon + U \left[\sum_{j\sigma'} \langle c_{j\sigma'}^\dagger c_{j\sigma'} \rangle - \langle c_{i\sigma}^\dagger c_{i\sigma} \rangle \right] - J \sum_{j \neq i} \langle c_{j\sigma}^\dagger c_{j\sigma} \rangle \right) c_{i\sigma}^\dagger c_{i\sigma} \quad (20)$$

Here we have assumed that the Hartree-Fock Hamiltonian has the same symmetry as the uncorrelated Hamiltonian, and hence off-diagonal expectation values $\langle c_{j\sigma'}^\dagger c_{i\sigma} \rangle$ for $(i\sigma) \neq (j\sigma')$ vanish. From this equation it is clear that the HF Hamiltonian can be written in terms of an effective one-particle energy

$$H = \sum_{i\sigma} \varepsilon_{i\sigma}^{\text{HFA}} c_{i\sigma}^\dagger c_{i\sigma} \quad (21)$$

where

$$\varepsilon_{i\sigma}^{\text{HFA}} = \varepsilon + U \left[\sum_{j\sigma'} \langle c_{j\sigma'}^\dagger c_{j\sigma'} \rangle - \langle c_{i\sigma}^\dagger c_{i\sigma} \rangle \right] - J \sum_{j \neq i} \langle c_{j\sigma}^\dagger c_{j\sigma} \rangle. \quad (22)$$

In the simple Hartree approximation (HA) the exchange decouplings are neglected, which means that all the decoupling terms with the negative sign would not occur. Therefore, the corresponding Hartree one-particle energies are given by

$$\varepsilon_{i\sigma}^{\text{HA}} = \varepsilon + U \sum_{j\sigma'} \langle c_{j\sigma'}^\dagger c_{j\sigma'} \rangle \quad (23)$$

Comparing this result with the Hartree-Fock one-particle energies, we find that the HF occupied levels are shifted downwards by an amount of

$$U \langle c_{i\sigma}^\dagger c_{i\sigma} \rangle + J \sum_{j \neq i} \langle c_{j\sigma}^\dagger c_{j\sigma} \rangle \quad (24)$$

relative to the Hartree levels. Momentarily setting $J = 0$, we see that for N occupied levels the Hartree approximation gives the one-particle energies

$$\varepsilon_{i\sigma}^{\text{HA}} = \varepsilon + NU \quad (25)$$

whereas the HFA yields

$$\varepsilon_{i\sigma}^{\text{HFA}} = \varepsilon + (N - 1)U . \quad (26)$$

The occupied Hartree-Fock one-particle energies are lower than the corresponding Hartree one-particle energies by U , which is a consequence of the artificial and unphysical self-interaction still present in the Hartree approximation that is exactly canceled in Hartree-Fock. This also explains why the Hartree-Fock bands are shifted downwards from the Hartree bands by an energy of the amount U . One also sees from this simple atomic-limit Hartree-Fock model that the energy difference between the highest occupied and the lowest unoccupied effective Hartree-Fock one-particle energies is again essentially U , which is once more in agreement with our numerical results for the crystal and for the atom (cf. Fig.6). Note that we have ignored U_{sd} interactions, which cause an additional shift of d-bands below the s-bands by about an additional 10 eV in the full HFA calculations.

Taking into account the exchange interaction J again and denoting by N_σ the number of occupied states with spin σ (i.e. $N = N_\uparrow + N_\downarrow$) one obtains in HFA

$$\varepsilon_\sigma^{\text{HFA}} = \varepsilon + (N - 1)U - (N_\sigma - 1)J . \quad (27)$$

Then the total energy in HFA is given by

$$E_{\text{tot}} = N\varepsilon + \frac{N(N - 1)}{2}U - \sum_\sigma \frac{N_\sigma(N_\sigma - 1)}{2}J . \quad (28)$$

For the total energy we have added the necessary correction term to the sum of the occupied energy levels (much like the double counting term that shows up in band-structure calculations). Now for partially filled 3d-shells the occupation of the different spin directions may be different. Denoting $M = N_\uparrow - N_\downarrow$ we obtain for the total energy

$$E_{\text{tot}} = N\varepsilon + \frac{N(N - 1)}{2}U - \frac{N^2 + M^2}{4}J + \frac{N}{2}J . \quad (29)$$

The magnetic ($M \neq 0$) total energy is lower than the non-magnetic (consistent with Hund's rules).

Take once more Co with 8 3d-electrons. The paramagnetic (non-magnetic) state has the occupations $N_\downarrow = N_\uparrow = 4$ ($N=8$ and $M=0$). For this configuration (corresponding to the left panel in Fig. 6) one obtains

$$E_{\text{tot}}^{(P)} = 8\varepsilon + 28U - 12J . \quad (30)$$

The Hund's rule magnetic solution has 3d-states of one spin-direction completely filled, i.e., $N_\uparrow = 5$ and $N_\downarrow = 3$ ($N=8$ and $M=2$). This gives

$$E_{\text{tot}}^{(M)} = 8\varepsilon + 28U - 13J . \quad (31)$$

Therefore, the magnetic configuration (with a magnetic moment of 2 for the atom) is energetically more favorable

by J . Note also the exchange splitting in the occupied energy eigenvalues

$$\varepsilon_\downarrow - \varepsilon_\uparrow = 2J \quad (32)$$

and that our model would predict the unoccupied minority spin E_{2g} state to be $U + J$ higher in energy than the corresponding occupied majority spin state.

The simple model in this section differs from the results shown in Fig. 6 in that we have replaced the full matrix of U and J by scalar values for d-states only (ignoring s-d interactions, for example). However, it captures all of the important physics without attempting to be completely quantitative.

VI. COMPARISON WITH LSDA AND EXX RESULTS

For comparison with the HFA results described in Section IV we have also performed a standard LSDA band-structure calculation with the LMTO-ASA method. We used the von Barth-Hedin exchange-correlation potential³⁹. Since these results are very similar to those of Ref. 26, we do not repeat them here. Again, our detailed results are given in Ref. 27. For the magnetic systems Fe, Co, and Ni we obtain an exchange splitting and the prediction of magnetic solutions with magnetic moments shown in Table V, which are in better agreement with experiment than the HFA results.

The energy spectra of the bands (DOS) are quite different from the HFA. For example, the 3d-bands now fall into the same energy region as the 4sp-bands, i.e., the LSDA-results are not so different from the Hartree-results. This means that the exchange-correlation energy leads only to a small shift of the 3d-bands downwards by at most a few eV and a smaller exchange splitting (also of the magnitude of 1 eV). On the other hand, in the LSDA calculations the self-interaction terms are not completely canceled, i.e., an (unrealistic) self-interaction is included, which may lead to 3d bands that lie energetically too high, as discussed for the atomic limit in the previous section.

To see the effect of correlations within LSDA, we have also performed an exchange-only calculation for Co, i.e. only the exchange part of the (local) exchange-correlation potential³⁹ was employed. The result is similar to the LSDA result, and the (majority) d-bands lie only about 1 eV lower than within LSDA, i.e., very minimal when compared with the large drop in the full HFA. This exchange-only LSDA-result also contains self-interactions, and their exact cancelation in the HFA is responsible for the large shift downwards of the d-bands. Nevertheless, the LSDA result indicates that a possible effect of correlations is to shift the 3d-bands up relative to exchange-only calculations, and hence one would expect a similar effect if correlations could be added to the full HFA calculations.

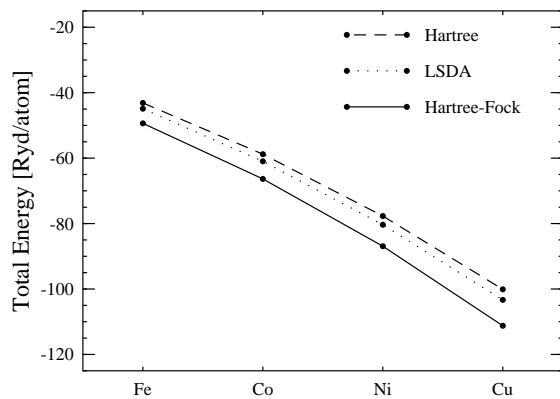


FIG. 7: Total ground state energy (of the valence electrons) obtained in Hartree-approximation, LSDA and HFA for the 3d transition metals Fe through Cu.

One can also calculate the total energy in the Hartree, HFA, and LSDA approximations. The results obtained for the four materials of interest are shown in Fig. 7. We see that the total energy is always significantly lower in HFA than in the Hartree approximation, which is expected because the HFA minimizes the total energy. The HFA total energy is also lower than the L(S)DA, and the LSDA result is lower than the simple Hartree result. Because of the unknown approximations that go into constructing L(S)DA, it is hard to guess ahead of time that this would be the case. However, it is well known that the L(S)DA approximation produces a bad total exchange-correlation energy; the reason why such good agreement with experiment is found is that relative exchange-correlation energies are nonetheless reasonably accurately calculated.

We now turn to the comparison of our results with exact exchange (EXX) calculations for 3d systems^{20,40}. This method, which is self-interaction-free, uses the EXX energy²⁰ instead of a LDA local exchange and then adds in a local LDA correlation potential. Like the HFA the magnetic moments for Fe, Co and Ni (see Table V) are overestimated by EXX⁴⁰. Our HFA results for Fe show the majority 3d-bands about 20 eV below the Fermi level (Fig. 1), whereas the EXX density of states (Fig. 2 in Ref. 20) show these bands only about 10 eV below the Fermi level. The differences are probably due to the (LDA) correlations shifting the 3d-bands upwards. This upward shift also occurs with EXX+RPA results in Ref. 40. Here the LDA correlations present in EXX are replaced by RPA correlations and the 3d-bands are found in the region of the 4sp-bands (similar to LDA). It is likely that the qualitative agreement between the HFA and EXX results for Fe is due to the correct cancelation of self-interactions.

VII. DISCUSSION AND CONCLUSION

We have presented the results of (unscreened) HFA calculations for the 3d transition metals Fe, Co, Ni and Cu. We obtain magnetic solutions for Fe, Co, and Ni with (slightly) too large magnetic moments when compared to experimental or LSDA results. The occupied HFA 3d-bands lie about 20 eV below the Fermi level (and the Hartree result), which is also the magnitude of the splitting between occupied and unoccupied 3d-bands and of the magnitude of the on-site Coulomb matrix element (the “Hubbard” U). This downwards shift of the HFA 3d-bands compared to the Hartree- and LSDA-3d-bands can be understood as due to the self-interaction correction of HFA.

One may argue that these results are not surprising and an artifact of using the unscreened HFA. Our ab-initio calculation of the direct Coulomb matrix elements yields large values of the magnitude of 20 eV. HFA can be considered to be an approximation for the selfenergy which is correct only in linear order in the Coulomb interaction. But for these large values of the U -terms HFA is certainly not sufficient but one has to apply better many-body approximations. One should apply systematic extensions of HFA, which within the standard perturbational approach can be represented by (a resummation of an infinite series of) Feynman diagrams, or one can try to apply the recently so successful non-perturbational many-body schemes like “dynamical mean field theory” (DMFT)⁴¹ or variational (Gutzwiller) approaches⁴². The simplest standard diagram series are the bubble diagrams leading essentially to the “random phase approximation” (RPA). This means just a renormalization of the interaction line, i.e. the pure “naked” Coulomb interaction has to be replaced by a “dressed” interaction. Or in other words, the exchange (Fock) contribution has not to be calculated with the bare Coulomb matrix elements but with screened Coulomb matrix elements. Probably the non-perturbational schemes like DMFT are also only applicable for screened Coulomb matrix elements.

We believe that the approach we have used for our HFA calculations can easily be generalized to provide an approach for combining ab-initio and many-body methods for the calculation of the electronic properties of solids. The starting point is a traditional band-structure calculation for an effective (auxiliary) one-particle Hamiltonian, which can be the Hartree-Hamiltonian. This yields, in particular, the eigenfunctions in the form of Bloch functions. Keeping only a finite number of J band indices restricts and truncates the Hilbert space for further calculations. We use the Marzari-Vanderbilt algorithm to construct maximally localized Wannier functions (within the truncated one-particle Hilbert space). All the one-particle (tight-binding) and two-particle (Coulomb) matrix elements between these Wannier functions can be calculated. The strong localization guarantees that only on-site matrix elements and near-neighbor inter-site matrix elements have to be calculated. We are left with a

many-body Hamiltonian in second quantization but with parameters determined from first principles for any given material, which we have solved within the HFA but for which we should also be able to solve by using more sophisticated many-body techniques. Our HFA approach is free from the problems of double counting of correlation effects and self-interaction and considers exchange contributions exactly. It does not rely on assumptions based on the homogeneous electron gas or a dependence on the local electron density. An inhomogeneous (lattice) electron system is considered right from the beginning. Within the standard Feynman diagram approach the most straightforward next step beyond HFA would be a summation of bubble diagrams leading to a renormalized (screened) Coulomb interaction. This would require calculating the exchange contribution not with the bare but with a screened Coulomb interaction. To take into

account the effects of screening would require a calculation of the charge susceptibility and the (static) dielectric constant, which could be done within a generalized Lindhard theory, for instance.

Acknowledgments

This work has been supported by a grant from the Deutsche Forschungsgemeinschaft No. Cz/31-12-1. It was also partially supported by the Department of Energy under contract W-7405-ENG-36. This research used resources of the National Energy Research Scientific Computing Center, which is supported by the Office of Science of the U.S. Department of Energy under Contract No. DE-AC03-76SF00098.

-
- ¹ P. Hohenberg, W. Kohn, Phys. Rev. **136**, B 864 (1964)
- ² R.M. Dreizler, E.K.U. Gross, *Density Functional Theory*, Springer (Berlin, Heidelberg, New York 1990)
- ³ H. Eschrig, *The Fundamentals of Density Functional Theory* (Teubner Stuttgart, Leipzig 1996)
- ⁴ W. Kohn, L.J. Sham, Phys. Rev. **140**, A1133 (1965)
- ⁵ J.H. Rose, J.R. Smith, F. Guinea and J. Ferrante, Phys. Rev. B **29**, 2963 (1984).
- ⁶ A. Svane, Phys. Rev. B **35**, 5496 (1986)
- ⁷ V.I. Anisimov, J. Zaanen, O.K.Andersen, Phys. Rev. B **44**, 943 (1991)
- ⁸ M.M. Steiner, R.C. Albers, D.J. Scalapino, L.J. Sham, Phys. Rev. B **43**, 1637 (1991)
- ⁹ M.M. Steiner, R.C. Albers, L.J. Sham, Phys. Rev. B **45**, 13272 (1992); Phys. Rev. Lett. **72**, 2923 (1994)
- ¹⁰ V.I. Anisimov, A.I. Poteryaev, M.A. Korotin, A.O. Anokhin, G. Kotliar, J. Phys. Cond. Matter **9**, 7359 (1997)
- ¹¹ A.I. Lichtenstein, M.I. Katsnelson, Phys. Rev. B **57**, 6884 (1998)
- ¹² V. Drchal, V. Janis, J. Kudrnovsky, Phys. Rev. B **60**, 15664 (1999)
- ¹³ M.I. Katsnelson, A.I. Lichtenstein, J. Phys. Cond. Matter **11**, 1037 (1999)
- ¹⁴ A. Liebsch, A. Lichtenstein, Phys. Rev. Lett. **84**, 1591 (2000)
- ¹⁵ T. Wegner, M. Potthoff, W. Nolting, Phys. Rev. B **61**, 1386 (2000)
- ¹⁶ I.A. Nekrasov, K. Held, N. Blümer, A.I. Poteryaev, V.I. Anisimov, D. Vollhardt, Eur. Phys. J. B **18**, 55 (2000)
- ¹⁷ Chapter 7 of Ref. 2
- ¹⁸ O. Gunnarsson, R.O. Jones, Physica Script. **21**, 394 (1980)
- ¹⁹ M. Stadel, J.A. Majewski, P. Vogl, A. Gorling, Phys. Rev. Lett. **79**, 2089 (1997)
- ²⁰ T. Kotani, H. Akai, Physica B 237-238, 332 (1997)
- ²¹ L. Hedin, B.I. Lundquist, Solid State Physics **23**, p.1 (Eds.: F. Seitz, D. Turnbull, H. Ehrenreich, Academic Press 1969)
- ²² For a recent review see: W. Aulbur, L. Jönsson, J.W. Wilkins in: Solid State Physics **54**, p.2 (Eds.: H. Ehrenreich, F. Spaepa, Academic Press 2000)
- ²³ N. Marzari and D. Vanderbilt, Phys. Rev. B **56**, 12847 (1997).
- ²⁴ O.K. Andersen, Phys. Rev. B **12**, 3060 (1975)
- ²⁵ H.L. Skriver, *The LMTO Method* (Springer-Verlag, Heidelberg 1984)
- ²⁶ V.L. Moruzzi, J.F. Janak and A.R. Williams, *Calculated Electronic Properties of Metals* (Pergamon, New York, 1978).
- ²⁷ I. Schnell, *Ab-initio Wannier Functions, Coulomb Matrix Elements, Hartree (-Fock) and LSDA Calculations for the 3d Transition Metals Fe, Co, Ni and Cu* Thesis at the University of Bremen, Germany (2002), available at: www-theorie.physik.uni-bremen.de/~ischnell/thesis
- ²⁸ G. Stollhoff, Phys. Rev. B **58**, 9826 (1998)
- ²⁹ G.D. Mahan, *Many-Particle Physics* (Plenum Press New York 1990)
- ³⁰ C. Pisani, R. Dovesi, C. Roetti, *Hartree-Fock Ab Initio Treatment of Crystalline Systems* (Lecture Notes in Chemistry, Vol. 48, Springer-Verlag Berlin Heidelberg 1988); C.Pisani, *Quantum-Mechanical Ab-initio calculation of the Properties of Crystalline Materials*, Lecture Notes in Chemistry, Vol. 67, Spinger Verlag, Heidelberg, 1996
- ³¹ H.J. Monkhorst, Phys. Rev. B **20**, 1504 (1979)
- ³² R.Dovesi, C. Pisani, F.Ricca, C.Roetti, Phys. Rev. B **25**, 3731 (1982)
- ³³ T. Kotani, Phys. Rev. B **50**, 14816 (1994)
- ³⁴ T. Kotani, Phys. Rev. Lett. **74**, 2989 (1995)
- ³⁵ I. Schnell, G. Czycholl, R.C. Albers, Phys. Rev. B **65**, 075103 (2002)
- ³⁶ J.C. Slater, Phys. Rev. **34**, 1293 (1929)
- ³⁷ R.E. Watson, Phys. Rev. **118**, 1036 (1959); **119**, 1934 (1959)
- ³⁸ L. Hodges, R.E.Watson, H.Ehrenreich, Phys. Rev. B **5**, 3953 (1972)
- ³⁹ U. von Barth and L. Hedin, J. Phys. C **5**, 1629-1642 (1972).
- ⁴⁰ T. Kotani, H. Akai, J. Magn. Magn. Mat. **177**, 569 (1998)
- ⁴¹ For a review see: A. George, G. Kotliar, W. Krauth, M.J. Rozenberg, Rev. Mod. Phys. **68**, 13 (1996)
- ⁴² W. Weber, J. Bünemann, F. Gebhard, in: *Band-Ferromagnetism* (Lecture Notes in Physics, Vol. 580, p.9 (eds.: K.Baberschke, M. Donath, W.Nolting, Springer Berlin 2001); J. Bünemann, W. Weber, F. Gebhard, Phys. Rev. B **57**, 6896 (1998)